

# Growth, Optical Characterization and Modeling of ZnO Nanorods on Si, SiC and Macroporous Si Structure

A. Ferreira da Silva<sup>1</sup>, M. V. Castro Meira<sup>1,2</sup>, J. A. Freitas Jr<sup>3</sup>, G. Baldissera<sup>4</sup>, C. Persson<sup>4</sup>, N. Gutman<sup>5</sup>, A. Sa'ar<sup>5</sup>, P. Klason<sup>6</sup>, M. Willander<sup>6,7</sup>

1- Instituto de Física, Universidade Federal da Bahia, Ondina, Salvador-Ba, 40210-340, Brazil

2- CETEC-Universidade Federal do Recôncavo da Bahia, Cruz das Almas - Ba, 44380-000, Brazil

3- Naval Research Laboratory ESTD, Washington, DC 20375-5347 USA

4- Department of Materials Science and Engineering, Royal Institute of Technology, SE-100 44 Stockholm, Sweden

5- Racah Institute of Physics and the Center for Nanoscience and Nanotechnology, the Hebrew University of Jerusalem, Jerusalem 91904 Israel

6- Department of Physics, Göteborg University, SE-412 96 Göteborg, Sweden

7- Department of Science and Technology (ITN), Linköping University, SE-601 74 Norrköping, Sweden

## ABSTRACT

Zinc Oxide (ZnO) and Silicon Carbide (SiC) are prominent materials with large applicability such as optoelectronic nanodevices and for instance ultraviolet detectors. There is lack of important information about optical transitions beyond the indirect band gap energy (BGE) of 4H-SiC and even more for ZnO direct BGE grown on the former material. Using vapor-liquid-solid and the aqueous chemical growth methods we have grown ZnO nanorods on different substrates, such as quartz, *n*- and *p*-type porous silicon, and *n*-type 4H-SiC. Scanning electron microscopy (SEM) was employed to compare sample morphologies. The absorption was calculated employing a projector augmented wave (PAW) method. The measured absorption of ZnO nanorods, on different substrates, is lower than that observed for ZnO films on quartz substrate, in the low energy spectral range. It is observed a strong effect of 4H-SiC substrates on ZnO nanorod properties. Experiment and theory show a good agreement when the shape of the optical absorption is considered for both materials.

**Keywords:** nanorods, ZnO, SiC, macroporous

## 1 INTRODUCTION

ZnO is of great interest due to its broad range of technological application such as optoelectronic nanodevices, biosensors, cosmetic and medicine [1-4]. It presents low toxicity and good chemical stability. This great versatility of applications is possible mainly because preparation conditions enhance different properties, such as, insulation, conductor, semiconductor, photo-electrochemical, luminescent, piezoelectric. In this work we have used ZnO nanopillars grown on two-dimensional macroporous periodic structure substrates of *n*- and *p*-type

Porous Silicon (PSi) and non-porous (flat) *n*- and *p*-type Si, and SiC [1].

SiC, a binary covalent inorganic material, is a semiconductor with physical and chemical properties values that excel that of silicon. Chips based on SiC can support very high temperatures and radiation without being affected or without losing information [5,6].

Photoacoustic spectroscopy (PAS) has been used to determine the optical absorption [7,8] of the ZnO films. First-principles projector augmented wave (PAW) method within the local density approximation (LDA), improved by an on-site Coulomb self-interaction potential (LDA+U) was employed to calculate the ZnO films absorption [9,10,11].

The properties of the ZnO films can be enhanced or implemented by the substrate characteristics. In this work, the photoacoustic technique was used to verify the influence of substrates in the absorption spectra of thin films of ZnO and luminescence techniques were employed to monitor the film properties.

## 2 EXPERIMENTAL PROCEDURES

### 2.1 Sample Preparation

Ordered arrays of trenches and holes in silicon substrates can be fabricated by either direct dry etching via masked substrates or by hydrofluoric (HF) acid based silicon electro-chemical etching. The later technique has the advantage of producing deep and uniform pattern of holes or pores that can be utilized to form two-dimensional (2D) and three-dimensional (3D) photonic crystals in silicon. Hence, we have utilized the fabrication techniques described in references [12, 13] to fabricate 2D pore arrays on top of *p*- and *n*-type silicon wafer. In brief, a standard photolithography followed by alkaline anisotropic etching has been used to define 2D pattern of inverted pyramids on top of silicon wafer. Electrochemical etching was

performed at room temperature in the dark for the *p*-type samples and under backside illumination for the *n*-type samples.

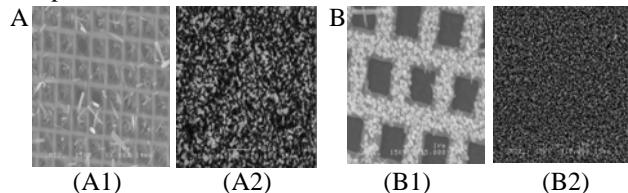


Fig.1 Scanning electron microscopy (SEM) images of *p*-PSi + ZnO (A) and *n*-PSi + ZnO (B) sample. Samples A1 and B1 are porous Si substrate samples. Samples A2 and B2 are flat Si substrate samples. All samples are grown with the ACG method.

ZnO nanopillars were grown on top of the silicon samples using an aqueous chemical growth method (ACG) and a vapor-liquid-solid method (VLS). There are several different chemical growth methods used to produce ZnO nanostructures. But the most common procedure is that described by Vayssieres *et al.* [14]. In this method zinc nitride ( $\text{Zn}(\text{NO}_3)_2 \cdot 6\text{H}_2\text{O}$ ) was mixed with hexamethylenetetramine (HMT  $\text{C}_6\text{H}_{12}\text{N}_4$ ). The substrates were placed in the solution and they were thereafter heated to 90°C for 180 minutes, upon which rods are formed on the substrate. An equi-molar concentration of HMT and zinc nitride (25 mM) was used.

In the VLS method, the ZnO powder was mixed with C powder using a 1:1 weight ratio. The mixture was loaded in a quartz boat and the Si substrate was mounted on top of the powder with a powder-substrate distance of 5 mm. The boat (with the ZnO:C powder and the Si substrate) was placed in the center of the furnace tube. Ar gas flow of 80 sccm was introduced for 5 minutes to stabilize the environment. The samples were grown for 30 minutes at 890°C.

## 2.2 Characterization Methods

PAS has been extensively used to determine the optical properties of semiconductor materials via energy transfer processes that results in heat generation [5,6]. The PAS consists in illuminating a given material with a modulated light beam and measuring the subsequent temperature fluctuation induced in the sample resulting from the light absorption, due to nonradiative de-excitation processes within the sample. The intermittent heat is transferred into the sealed gas chamber generating an acoustical signal that can be detected by a microphone. The light source of the PAS comprise of a high-pressure 1000W xenon arc lamp (Osram), modulated to 20 Hz by a chopper (HMS Elektronik, model 220A) and a scanning monochromator (Sciencetech, model 9010). The spectra were acquired in the spectral region from 350 nm to 700 nm, corresponding to energies from 3.54 eV to 1.77 eV. The light absorbed by the sample, which replaces the cell exit window (the ZnO film side was turned toward the cell cavity), produces a

photoacoustic signal, which is detected by a microphone attached to the cell. This microphone is connected to a Lock-in amplifier (Stanford Research System, model SR530), which synchronizes the PA signal with the reference pulse from the chopper. Band-band pass optical filters were employed to eliminate the contribution from the second order of diffraction, for wavelength smaller than 570 nm. The sample luminescence was excited at room with the unfocused 325 nm line of a HeCd laser. The uncorrected photoluminescence (PL) spectra were obtained with a fiber optical spectrometer, comprised of an UV extended linear array and a grating blazed at 350 nm, coupled to a near-UV transmitting inverted optical microscope. Real-color and single color optical images, acquired with different magnifications, were obtained with a near-UV CCD fitted with a wheel filter attached to one of the microscopes ports. Both the PL spectra and the luminescence images were excited with laser power density of about 10 mW/cm<sup>2</sup>.

## 3 RESULTS

To verify the influence of substrates on the optical properties of ZnO films, we carried out experiments on films deposited on *n*- and *p*-type non-Porous silicon (Si) and Porous Silicon (PSi), and on *n*-type 4H:SiC. Bulk ZnO wafer was measured to obtain references. This latter yielded an energy gap around  $E_g = 3.09$  eV. The samples of silicon *p*-type (*p*-Si and *p*-PSi) and *n*-type Si (*n*-Si and *n*-PSi) show a broad band of absorption between 400 nm and 680 nm.

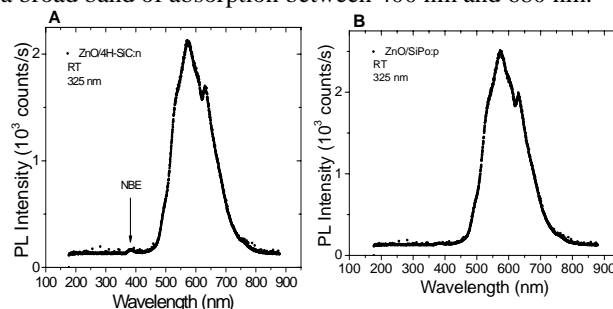


Fig. 2 (a) RT PL spectrum of ZnO film deposited on 4H:SiC substrate. The small peak at 383nm is assigned to the ZnO NBE emission. (b) RT PL spectrum of ZnO film grown on *p*-type porous Si.

Photoluminescence spectra were acquired for most of the samples. Fig. 2a and 2b depict the PL spectra of films deposited on 4H-SiC and *p*-type porous Si, respectively. They are characterized by a dominant and broad emission band extending between 450 and 800 nm, with peak around 575 nm. In addition, a weak peak is observed around 383 nm, which is close to 379 nm, the near band edge emission (NBE) peak observed in high-quality bulk ZnO sample, measured under identical condition. The 575 nm broad emission band peaks at longer wavelength than that of the bulk ZnO at ~ 510 nm. The latter has been assigned to recombination process involving electrons trapped at a

single oxygen vacancy with photo-generated holes [15]. Additional experiments must be performed to obtain insights about that nature of the broad band, which may have more than one component. The observation of the NBE emission is consistent with the deposition of good quality ZnO films. The small strength of the peak may result from the low power excitation condition, which favor the long time recombination processes associated with the broad emission band. Measurements with different excitation conditions and temperature will be carried out.

Calculations for optical absorption of ZnO were based on the density function theory within the LDA, employing the scalar-relativistic PAW method [9]. The LDA band-gap energy was corrected self-consistently with an on-site Coulomb potential within the LDA+U approach [9,10,11] with  $U_d(\text{Zn}) = 4$  eV. The correction of the Zn  $d$ -states within LDA+U have been found [16] to significantly improve the  $\text{Zn}_d\text{-O}_p$  hybridization at  $\sim 7$  eV below the valence band maximum. The underestimate LDA+U band gap is corrected according to Ref. [16]. Moreover, we expect a downward band-gap shift by 0.1-0.2 eV due to temperature effects.

In order to obtain the absorption coefficient we calculated first the dielectric functions  $\epsilon(\omega) = \epsilon_1(\omega) + i\epsilon_2(\omega)$ . The imaginary part of the dielectric function,  $\epsilon_2(\omega)$ , in the long wavelength limit,  $\epsilon_2(\omega) = \text{Im}[\epsilon(q = 0, \omega)]$ , has been obtained directly from the electronic structure, using the joint density-of-states and the optical matrix overlap:

$$\epsilon_2^{ij}(\omega) = \frac{4\pi^2 e^2}{\Omega m^2 \omega^2} \sum_{\mathbf{k}n\sigma} \langle \mathbf{k}n\sigma | p_i | \mathbf{k}n'\sigma \rangle \langle \mathbf{k}n'\sigma | p_j | \mathbf{k}n\sigma \rangle f_{\mathbf{k}n}(1 - f_{\mathbf{k}n'}) \delta(e_{\mathbf{k}n'} - e_{\mathbf{k}n} - \eta\omega) \quad (1)$$

where  $e$  is the electron charge,  $m$  its mass,  $\Omega$  is the crystal volume and  $f_{\mathbf{k}n}$  is the Fermi distribution. Moreover,  $|\mathbf{k}n\sigma\rangle$  is the crystal wave function corresponding to the  $n$ th eigenvalue  $e_{\mathbf{k}n}$  with crystal momentum  $\mathbf{k}$  and spin  $\sigma$ . The summation over the irreducible Brillouin zone in Eq. (1) has been calculated using the tetrahedron interpolation with a  $\mathbf{k}$ -mesh consisting of about 450 uniformly distributed  $\mathbf{k}$ -points. The real part of the dielectric function,  $\epsilon_1(\omega)$ , is obtained from  $\epsilon_2(\omega)$  using the Kramers-Kronig relation

$$\epsilon_1(\omega) \equiv \text{Re}(\epsilon(q=0, \omega)) = 1 + \frac{1}{\pi} \int_0^\infty d\omega' \epsilon_2(\omega') \left( \frac{1}{\omega' - \omega} + \frac{1}{\omega' + \omega} \right) \quad (2)$$

The absorption coefficient  $\alpha(\omega)$  is obtained from

$$\epsilon_1^2(\omega) + \epsilon_2^2(\omega) = [e_1(\omega) + \alpha^2(\omega)c^2 / 2\omega^2]^2$$

The shape of the calculated LDA+U absorption spectrum of ZnO agree qualitatively well with measured spectrum

Optical transition around 3.2eV was observed in most of the ZnO films deposited on those substrates. However, no

absorption features were observed for  $n$ -PSi+ZnO, whose thickness of the film is smaller than  $1\mu\text{m}$ .

To determine the energy gap of these materials, we have used two methods [18,19]: Linear and Derivative. The first method, the relationship  $I(h\nu) = A(h\nu - E_g)^{1/2}$  was used because the material has a direct optical transition.  $I$  is the intensity of the absorption,  $h\nu$  is a energy of photons and  $E_g$  is obtained by linear extrapolation of the best fit between  $(I(h\nu))^2$  and  $h\nu$  at the point where it meets the axis of the energy [19,20], as represented in Fig. 3. The latter method is the derivative from the experimental points that compose the absorption spectrum. This operation brings up the critical points of the spectrum corresponding to the peaks of the numerical derivative. A careful review of the position of each peak gives the energy of forbidden band. Note that, for this method the energy of the energy is higher than determined by the Linear Method.

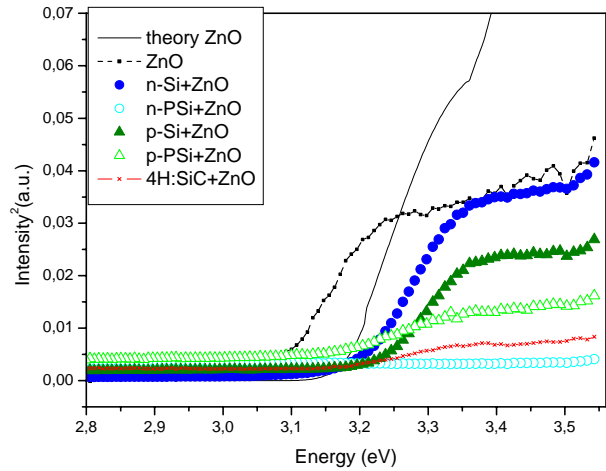


Fig. 3 Photoacoustic absorption spectra of the samples ZnO,  $n$ -Si+ZnO,  $n$ -PSi+ZnO,  $p$ -Si+ZnO,  $p$ -PSi+ZnO and 4H:SiC+ZnO, and the theoretical model (DFT) [17] result for zinc oxide film absorption.

Note that, the energy gap values obtained from the Linear and Derivative theoretical methods (Table 1) and the experimental data ( $E_g = 3.09$  eV) differ in less than 1%. Also, note that the measured value of 3.17 eV for the energy gap of the 4H:SiC+ZnO sample is close to that of 4H-SiC proposed by Astrath et al. [21], i.e., about 3.2 eV. This may be expected for a thin ZnO film, deposited on 4H-SiC, an indirect band gap material, with the direct band gap near 6.0 eV. The results using the photoacoustic technique are compatible with those reported in the specialized literature.

For  $n$ -type PSi, no enhancement around the  $E_g$  of ZnO was observed. Probably due to the columnar like formation of the ZnO film on the  $n$ -type PSi substrate, differently from  $p$ -type PSi that has a thin sponge-like morphology continuous film. [22]

|                              | Linear Method | Derivative Method | Discrepancy |
|------------------------------|---------------|-------------------|-------------|
| Theory ZnO                   | 3.16 eV       | 3.15 eV           | 0.31%       |
| Experiment ZnO               | 3.09 eV       | 3.14 eV           | 1.6%        |
| Experiment <i>N</i> -Si+ZnO  | 3.21eV        | 3.27eV            | 1.8%        |
| Experiment <i>P</i> -Si+ZnO  | 3.21 eV       | 3.28 eV           | 2.1%        |
| Experiment <i>P</i> -PSi+ZnO | 3.09 eV       | 3.24 eV           | 4.6%        |
| Experiment 4H:SiC+ZnO        | 3.17 eV       | 3.30 eV           | 4.0%        |

Table 1: Comparison between the Linear and Derivative Method for determination of energy gap.

## 4 CONCLUSION

ZnO nanopillars were successfully grown using both the ACG and VLS method on n- and p-type plane and porous Si. PL results indicate that ZnO films were deposited on these substrates. The optical absorption measured from all samples, using Photoacoustic spectroscopy, was compared with a bulk ZnO wafer and the calculated absorption. The calculations were performed within the PAW method using the local density approximation improved by an on-site Coulomb self-interaction potential.

The theoretical results show good agreement with experimental data. It was not possible to observe the optical transition assigned to the ZnO film deposited on the n-PSi+ZnO substrate, because its small thickness. Extremely high frequency modulation experiments are required to probe very thin films. The value of the energy gap of the samples *n*-Si+ZnO and *p*-Si+ZnO, obtained by the photoacoustic technique, shifted to the ultra-violet spectral region as compared with the theoretical and experimental data of ZnO. Additional experiments are planned to investigate the mechanism associated with this shift.

## ACKNOWLEDGMENTS

The authors acknowledge the financial support of the Brazilian agencies FAPESB/PRONEX and CNPQ, the Swedish Energy Agency (STEM), the Swedish Research Council (VR), and the European EM ECW Programme.

## REFERENCES

[1] S. M. Al-Hilli, R. T. Al-Mofarji, P. Klason, M. Willander, N.Gutman and A. Sa'ar, J.App.Phys, 103, 014302, 2008.  
[2] G. Zheng, F. Patolsky, Y. Cui, W. U. Wang and C. M Lieber, Nat. Biotechnology. 23, 1294, 2005  
[3] S. Al-Hilli, A. Öst, P. Stalfors and M. Willander, J. Appl. Phys 102, 084304, 2007

[4] S. M. Al-Hilli, R. T. Al-Mofarji, and M. Willander, Appl. Phys. Lett. 89, 173119, 2006  
[5] C. Persson and A. Ferreira da Silva, in "Optoelectronic Devices: III-Nitrides" (Elsevier, Oxford, 2004), pp. 479-559.  
[6] A. Ferreira da Silva, J. Pernot, S. Contreras, B.E.Sernelius, C. Persson, J.Camassel, Phys. Rev B 74, 245201, 2006.  
[7] A. Ferreira da Silva, N. Veissid, C. Y. An, I. Pepe, N. Barros de Oliveira, and A. V. Batista da Silva, Appl. Phys. Lett. 69, 1930, 1996  
[8] J. L. Gole, E. Veje, R. G. Egeberg, A. Ferreira da Silva, I. Pepe and D. A. Dixon, J. Phys. Chem. B 110, 2064, 2006  
[9] G. Kresse and J. Joubert, Phys. Rev. B 59, 1758 (1999)  
[10] P.E. Blöchl, Phys. Rev. B 50, 17953, 1994  
[11] C. Persson and A. Ferreira da Silva, Appl. Phys. Lett. 86, 231912, 2005  
[12] V. Lehmann, H. Föll, J. Electrochem. Soc. 137, 653, 1990  
[13] V. Lehmann, U. Grüning. Thin Solid Films 297, 13, 1997  
[14] L. Vayssieres, K. Keis, S.E. Lindquist, A. Hagfeldt, J. Phys. Chem. B 105, 3350, 2001  
[15] Y. Chen, K. Kong, H.J. Ko, M. Nakajima, T. Yao, Y. Segawa, Appl. Phys. Lett. 76, 245, 2000  
[16] C.Persson, C.L.Dong, L.Vayssieres, A.Augustsson, T.Schmitt, M.Mattesini, R.Ahuja, J.Nordgren, C.L.Chang, A.Ferreira da Silva, J.-H.Guo, Microelectron. J. 37, 686, 2006  
[17] C.Persson, C.Platzer-Björkman, J.Malmström, T.Törndahl, M.Edoff, Phys. Rev. Lett. 97,146403, 2006  
[18] J. Singh, "Physics of Semiconductors and their Heterostructures", McGraw-Hill series in electrical and computer engineering, New York, 1993.  
[19] J.I. Pankove, "Optical Processes in Semiconductors", Dove Publications, New York, 1975.  
[20] R.H. Bube. "Photoelectronic Properties of Semiconductors"; Cambridge University Press. Cambridge, England, 1992.  
[21] N.G.C.Astrath, A.C.Bento, M.L.Baesso, A.Ferreira da Silva, C.Persson, Thin Solid Films, 4, 515, 2006.  
[22] A.Beloto, M.Ueda, E.Abramof, J.R.Senna, M.D.Silva, C.Kuranaga, H.Reuther, I.Pepe, A.Ferreira da Silva, Surface and Coatings Technology 156, 267, 2002.